Selective methioninase-induced trap of cancer cells in S/G_2 phase visualized by FUCCI imaging confers chemosensitivity

Shuya Yano[1,2,3], Shukuan Li[1], Qinghong Han[1], Yuying Tan[1], Michael Bouvet[2], Toshiyoshi Fujiwara[3] and Robert M. Hoffman[1,2]

[1] AntiCancer, Inc, San Diego, CA

[2] Department of Surgery, University of California, San Diego, CA

[3] Department of Gastroenterological Surgery, Okayama University Graduate School of Medicine, Dentistry and Pharmaceutical Sciences, Okayama, Japan

Correspondence to: *Robert M. Hoffman,* ***email:*** *all@anticancer.com*

Keywords: cell cycle, FUCCI, imaging, S/G_2 phase block, recombinant methioninase, rMETase, chemotherapy, HeLa cells, MCF-7 cells

Received: *July 18, 2014* ***Accepted:*** *August 18, 2014* ***Published:*** *August 19, 2014*

ABSTRACT

A major impediment to the response of tumors to chemotherapy is that the large majority of cancer cells within a tumor are quiescent in G_0/G_1, where cancer cells are resistant to chemotherapy. To attempt to solve this problem of quiescent cells in a tumor, cancer cells were treated with recombinant methioninase (rMETase), which selectively traps cancer cells in S/G_2. The cell cycle phase of the cancer cells was visualized with the fluorescence ubiquitination cell cycle indicator (FUCCI). At the time of rMETase-induced S/G_2-phase blockage, identified by the cancer cells' green fluorescence by FUCCI imaging, the cancer cells were administered S/G_2-dependent chemotherapy drugs, which interact with DNA or block DNA synthesis such as doxorubicin, cisplatin, or 5-fluorouracil. Treatment of cancer cells with drugs only, without rMETase-induced S/G_2 phase blockage, led to the majority of the cancer-cell population being blocked in G_0/G_1 phase, identified by the cancer cells becoming red fluorescent in the FUCCI system. The G_0/G_1 blocked cells were resistant to the chemotherapy. In contrast, trapping of cancer cells in S/G_2 phase by rMETase treatment followed by FUCCI-imaging-guided chemotherapy was highly effective in killing the cancer cells.

INTRODUCTION

The problem of quiescent cancer cells within a tumor

The resistance of most solid tumors and metastases is a major problem in chemotherapy. The phase of the cell cycle determines to a great extent whether a cancer cell can respond to a given drug. We previously monitored real-time cell cycle dynamics of cancer cells throughout a live tumor intravitally using a fluorescence ubiquitination cell cycle indicator (FUCCI). Approximately 90% of cancer cells in the center and 80% of total cells of an established tumor are in G_0/G_1 phase. Similarly, approximately 75% of cancer cells far from (> 100 μm) tumor blood vessels of an established tumor are in G_0/G_1. FUCCI imaging demonstrated that cytotoxic agents killed only proliferating cancer cells at the surface, or near blood vessels, and had little effect on the majority of quiescent cancer cells within a tumor. Resistant quiescent cancer cells restarted cycling after the cessation of chemotherapy. Thus, the low chemo-sensitivity of most solid tumors is at least in part due to the large majority of cancer cells in solid tumors being quiescent [1].

FUCCI imaging was used for real-time visualization of the cell cycle kinetics of invading cancer cells in 3-dimensional (3D) Gelfoam® histoculture. Cancer cells in G_0/G_1 phase in Gelfoam® histoculture migrated more rapidly and further than the cancer cells in $S/G_2/M$ phase. After entry into $S/G_2/M$ phases, cancer cells ceased

migrating and restarted migrating after division when the cells re-entered G_0/G_1. Migrating cancer cells were resistant to cytotoxic chemotherapy, since they were mostly in G_0/G_1 [2].

One solution to the problem of large numbers of cells in G_0/G_1 in a tumor is to block the cancer cells in S/G_2 rather than G_0/G_1.

Methionine dependence

Methionine dependence, the elevated methionine requirement for cancer cell proliferation, is the property of the majority of cancer cell types [3]. There have been several therapeutic strategies to target the methionine dependence of cancer cells. Methionine-starvation therapy, such as with a methionine-free diet or methionine-depleted total parenteral nutrition, prolonged the survival time of tumor-bearing rodents [4, 5]. Methionine-free total parenteral nutrition in combination with chemotherapeutic drugs extended the survival of patients with high-stage gastric cancer [4]. Prostate-cancer patients have been treated with a methionine-depleted diet [5].

A reversible growth arrest of cancer cells has been produced by replacement of methionine in the growth medium by its immediate metabolic precursor, homocysteine, This growth arrest is accompanied by a reduction in the percentage of mitotic cells in the cell population. Furthermore, fluorescence-activated cell sorting demonstrated that the cells are arrested at the S/G_2 phase of the cell cycle. This is in contrast to a G_1-phase accumulation of cancer cells, which occurs only in methionine-supplemented medium at very high densities and which is similar to the G_1 block seen in cultures of normal fibroblasts at high density [6]. The molecular mechanism of the S/G_2 block has subsequently been investigated [7].

The S/G_2 trap that that cancer cells enter upon methionine starvation was exploited for selective chemotherapy *in vitro*. In cultures that were initiated with equal amounts of cancer cells and human diploid fibroblasts, substitution of homocysteine and doxorubicin for methionine in the culture medium followed by methionine repletion with vincristine was totally effective at selectively eliminating a methionine-dependent human sarcoma and three methionine-dependent human carcinomas. This chemotherapeutic procedure used was not toxic to normal cells growing alongside the cancer cells and was ineffective when conducted totally in methionine-containing medium [8].

In the present report, we demonstrate that using recombinant methioninase (rMETase) to deplete methionine and thereby trap cancer cells in S/G_2, and FUCCI imaging to detect the onset of the block, chemotherapy could become effective on the S/G_2-trapped cancer cells.

RESULTS AND DISCUSSION

Recombinant methionine (rMETase) block of cancer cells in S/G_2 visualized by FUCCI imaging

After seeding on 35 mm glass dishes and culture over night, HeLa cells were treated with rMETase at a dose of 1.0 unit/ml. rMETase blocked HeLa and MCF-7 cells in the S/G_2 phase of the cell cycle as visualized by FUCCI imaging (Figure 1).

After seeding on 35 mm glass dishes and culture over night, HeLa and MCF-7 cells were treated with rMETase either at 0.25 or 0.5 units/ml for 48 hours. FUCCI imaging showed that by 24 hours there was a large shift in the cancer-cell population from G_0/G_1 to $S/G_2/M$ (Figure 2). For HeLa cells, the percentage of cells in G_0/G_1 decreased from approximately 80% to approximately 20%

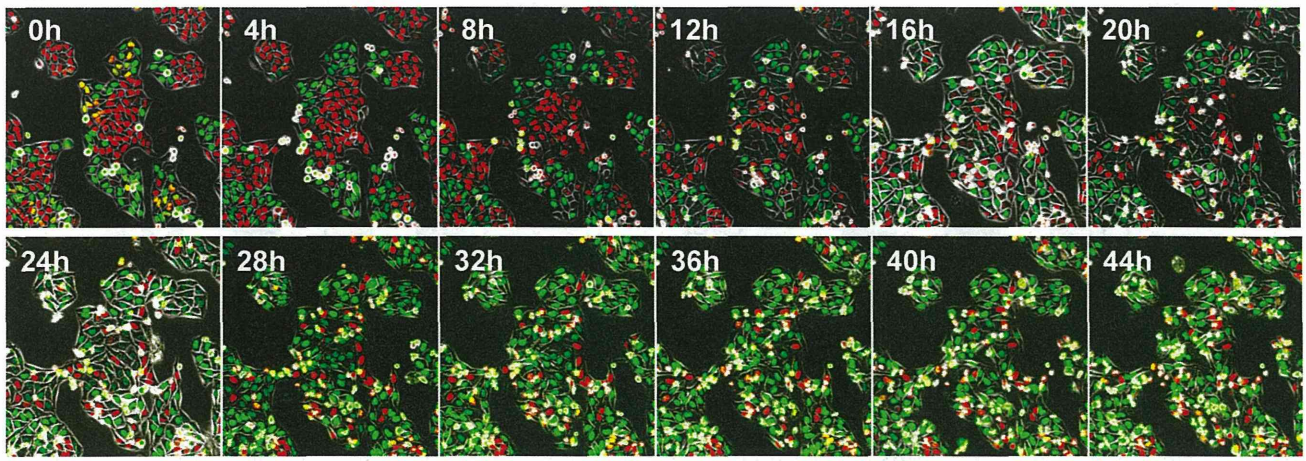

Figure 1: Time-lapse imaging of FUCCI-expressing HeLa cells treated with rMETase. After seeding on 35 mm glass dishes and culture over night, HeLa cells were treated with rMETase at a dose of 1.0 unit/ml. All images were acquired with the FV1000 confocal microscope (Olympus, Tokyo, Japan). The cells in G_0/G_1, S, or G_2/M phases appear red, yellow, or green, respectively. Scale bar: 50 μm.

by 48 hours in the presence of either 0.25 or 0.5 units/ml rMETase. Approximately 80% of the population became blocked in S/G_2. For MCF-7 cells, approximately 40% of the untreated cells were in G_0/G_1. After 48 hours treatment with 0.25 units/ml rMETase, the percentage of cells in G_0/G_1 fell to 20% and with 0.5 units rMETase, the percentage decreased to approximately 15%. Approximately 85% of the cells became trapped in S/G_2 (Figure 2).

Cytotoxic chemotherapy drugs killed cancer cells trapped in S/G_2 by rMETase

During rMETase-induced blockage in S/G_2, doxorubicin (DOX) effectively killed the cancer cells. After overnight culture, HeLa cells and MCF-7 cells were treated with 0.25 unit/ml rMETase for 48 hours. The cancer cells were then treated with 0.5 μg/ml DOX (HeLa cells) or 2.5 μg/ml DOX (MCF-7) for 72 hours. HeLa cells were also treated with 0.5 μg/ml DOX, and MCF-7 cells were treated with 2.5 μg/ml DOX for 72 hours, both without rMETase. With HeLa cells, DOX treatment alone resulted in an increase of cells in G_0/G_1 from approximately 60% to 80%. With combination treatment of DOX and rMETase, the number of HeLa cells in G_0/G_1 was reduced to approximately 0 with almost all cells blocked in S/G_2. For MCF-7 cells, approximately 40% of the untreated cells were in G_0/G_1 and increased to more than 80% after treatment with DOX alone for 72 hours. In the presence of rMETase and DOX for 72 hours, approximately 40% of the cells were in G_0/G_1 (Figure 3).

DOX alone, at 2.5 μg/ml, killed approximately 25% of the MCF-7 cells. The combination of DOX, at 2.5 μg/ml, and rMETase, at 0.25 units/ml, killed approximately 80% of the cells ($P<0.01$ compared to DOX alone). DOX, at 5 μ/ml, and rMETase, at 0.25 units/ml, killed approximately 90% of the cells ($P<0.01$ compared to DOX alone) (Figure 4).

For MCF-7 cells treated with 5-FU, at 15 μg/ml, approximately 40% of the cells were killed. With the combination of rMETase (0.25 units/ml) and 15 μg/ml 5-FU, approximately 80% of the cells were killed ($P<0.01$ compared to 5-FU alone). With 5-FU, at 30 μg/ml, approximately 40% of the cells were killed, and the combination of 5-FU, at 30 μg/ml, and 0.25 units/ml rMETase, approximately 90% of the cells were killed

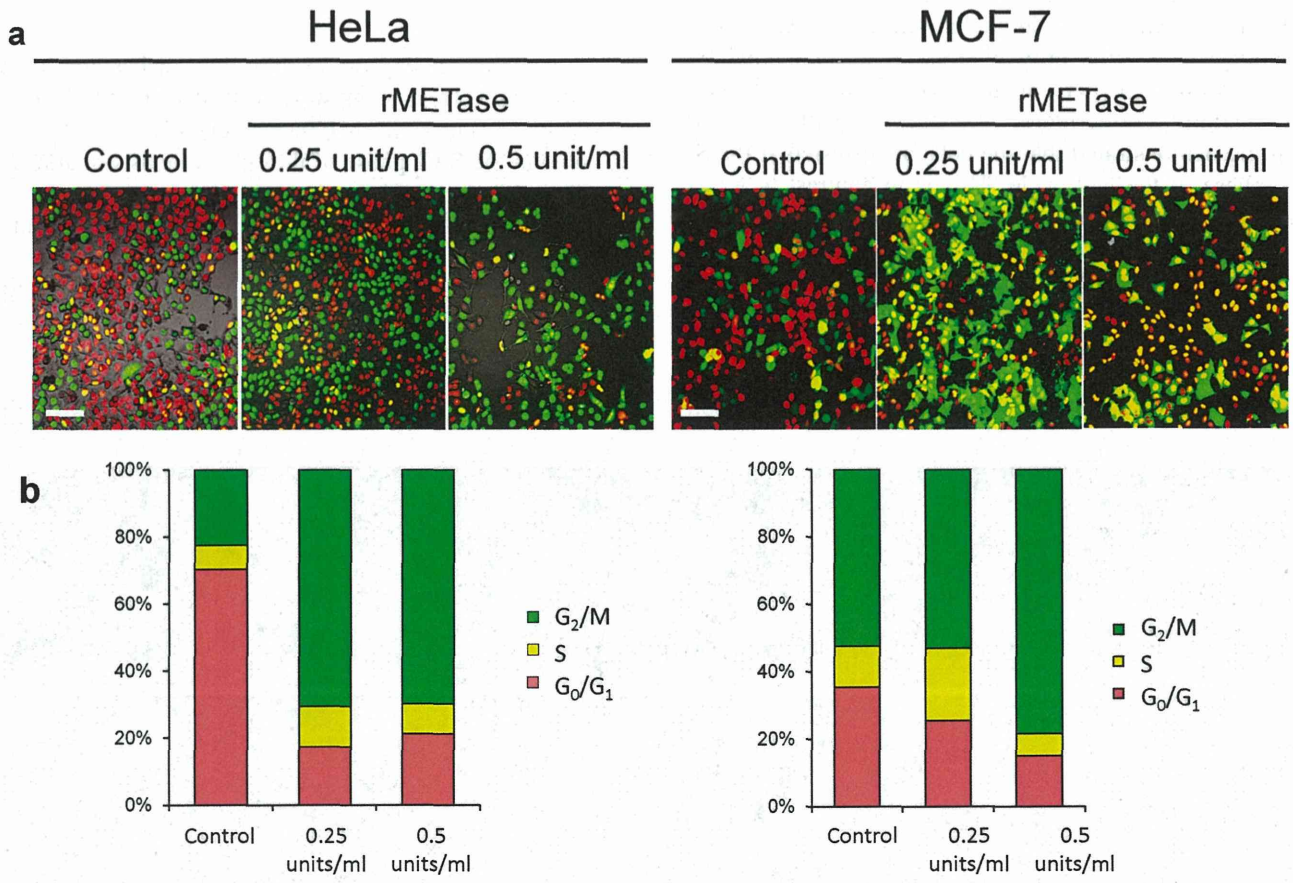

Figure 2: rMETase traps cancer cells in S/G_2 phase. After seeding on 35 mm glass dishes and culture over night, HeLa cells and MCF-7 cells were treated with rMETase, at the indicated doses, for 48 hours. a. Representative images of control or rMETase-treated cells. b. Histogram shows the percentages of cells in G_1 (red), early S (yellow), or late $S/G_2/M$ (green). Cells at each cell cycle phase were quantitatively assessed by counting the number of cells with each color. N=5 experiments were analyzed. Scale bars: 50 μm.

(P<0.01 compared to 5-FU alone) (Figure 4).

The strategy and technology described in this report, whereby cancer cells are selectively and synchronously trapped by rMETase in S/G_2, the most drug-sensitive phase of the cell cycle, where they were identified by FUCCI imaging and then treated with S/G_2-phase-specific-drugs was highly effective compared to standard chemotherapy.

Previously developed concepts and strategies of highly selective tumor-targeting [9-20] can take advantage of spatial–temporal cell-cycle imaging of cancer cells described in the present and previous [1, 2, 21] reports.

Previously, different methods of cancer-cell synchronization have been used in order to sensitize the cells to chemotherapy. Such methods include

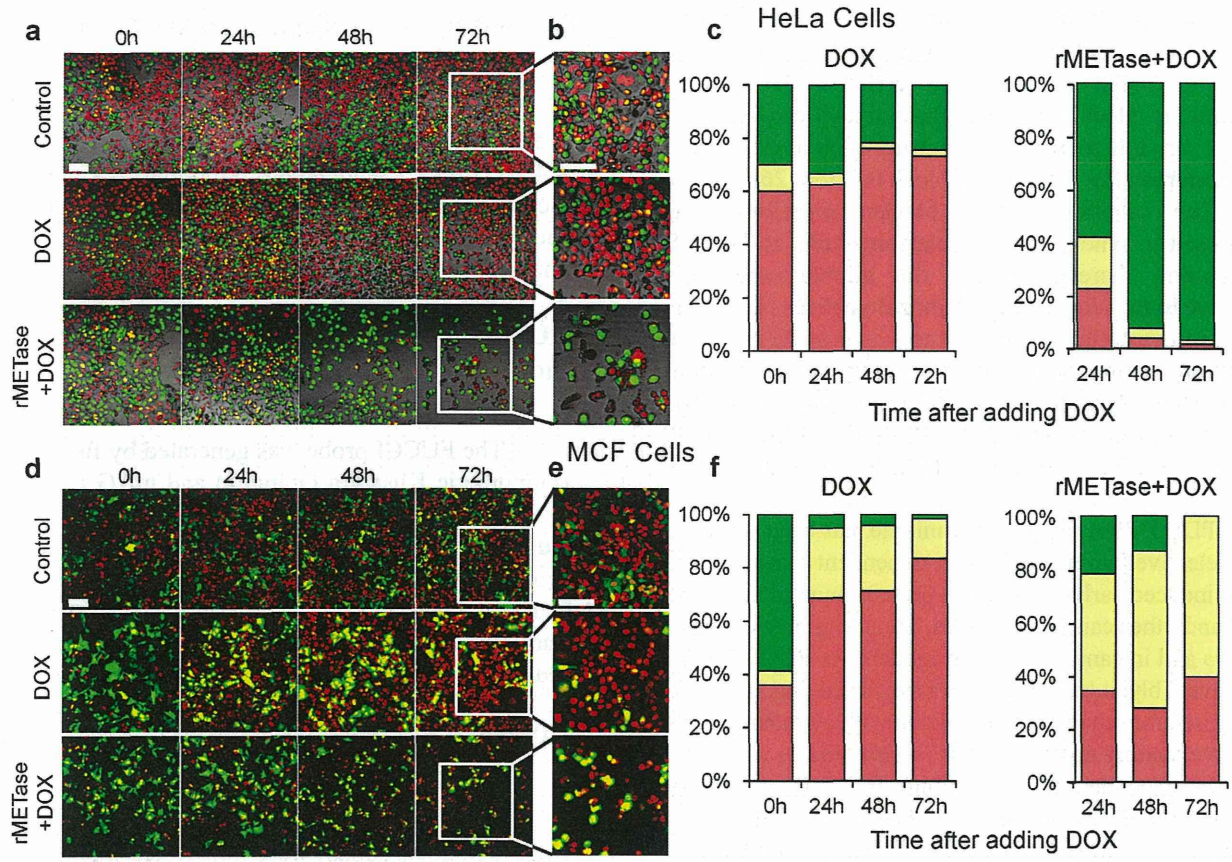

Figure 3: FUCCI cell cycle analysis during chemotherapy with and without rMETase. After overnight culture, HeLa cells (a, b and c) and MCF-7 cells (d, e and f) were treated with 0.25 unit/ml rMETase for 48 hours and, then were treated with 0.5 μg/ml doxorubicin (HeLa cells) or 2.5 μg/ml doxorubicin (MCF-7) for 72 hours. For conventional chemotherapy, after culture for 48 hours, HeLa cells (a, b and c) and MCF-7 cells (d, e and f) were treated with 0.5 μg/ml DOX (HeLa cells) or 2.5 μg/ml DOX (MCF-7) for 72 hours. a, b, d, e Representative images acquired with the FV-1000 are shown. c, f, Histograms show the percentages of cells G_1(red), early-S (yellow), or late-S/G_2/M (green). Cells at each cell cycle phase were quantitatively assessed by counting the number of cells with each color. N=5 experiments were analyzed. Scale bars: 50 μm.

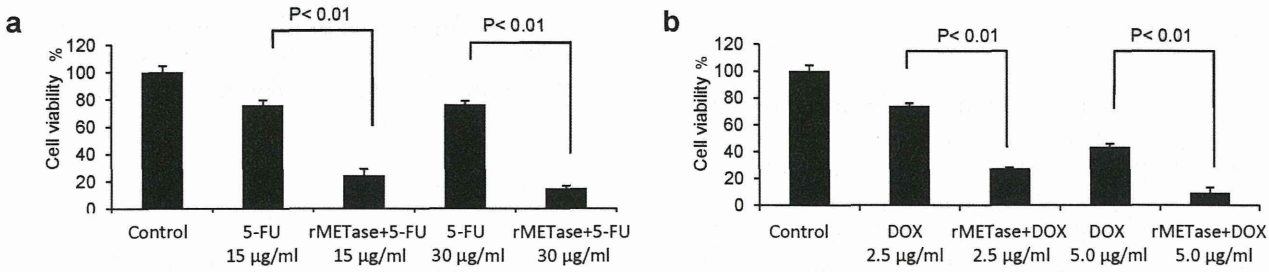

Figure 4: Chemotherapy of S/G_2-trapped cancer cells. Efficacy of combination therapy of rMETase and 5-FU (a); rMETase and DOX (b); on FUCCI-expressing MCF-7 cells. Cell viability was assessed by counting living cells compared to control. Data bars means ± SD of triplicate samples.

chronotherapy which attempts to target the time of day when most cancer cells in tumors are thought to be dividing [22]. Excess thymidine or its analogs have also been used to arrest cancer cells in S-phase, where they are sensitized to S-phase drugs such as 5-FU or methotrexate, and after release of the block, the cancer cells enter M-phase synchronously where they are sensitive to M-Phase drugs such as paclitaxel [23-25].

Cancer-cell synchronization with cell-cycle-phase-specific drugs, such as cytosine arabinoside, methotrexate and hydroxyorea have also been carried out [26-30], for example, to block cells in S-phase which can sensitize the cancer cells to an M-phase drug, such as paclitaxel, administered after the S-phase block is lifted [26-30].

The calcium channel blocker mibefradil has been used to synchronize glioblastoma cells at the G_1/S checkpoint, thereby making the glioblastoma cells sensitive to first-line therapy temozolomide [31]. Statins, such as Lovastatin, can be used to synchronize cancer in G_1 by preventing formation of an early intermediate in the cholesterol pathway essential for progression of cells through early G_1 phase [32, 33]. After the block is lifted, the cancer cells can be effectively treated with an S-phase drug.

PDO332991, a pyridopyrimidine, has been shown to be a selective inhibitor of cyclin-dependent kinases 4 and 6 and induced early-G_1 arrest in primary human myeloma cells and other cancer cell types, including breast cancer *in vitro* and in cancer xenograft models. As PDO0332991 acts reversibly, it can be used as a synchronizing agent and when used for sequence combination with cytotoxic agents is active against myeloma cells *in vitro* and *in vivo* [34]. A cyclin-dependent kinase inhibitor RO-3306 reversibly arrests 95% of treated cells in G_2 phase. These cells rapidly enter mitosis after the block is lifted and become sensitive to M-phase drugs [35]. Growth factors such as EGF, G-CSF, and IL-6 can stimulate cancer cell out of G_0, making them sensitive to chemotherapy agents such as docetaxel [36-38]. Reviews on cell synchronization are available [39-42].

The critical advantage of rMETase synchronization (blockage) is that, unlike the methods described above, it is cancer specific [3,6,8,43-51].

CONCLUSIONS

A major problem for successful chemotherapy is the very high percentage of quiescent G_0/G_1 cancer cells in a tumor. The present report has demonstrated a solution to the problem by selectively trapping cancer cells in S/G_2, with recombinant methioninase (rMETase). The S/G_2-trapped cancer cells became sensitive to chemotherapy which targets cells in this phase of the cell cycle, which are the majority of the most widely-used chemotherapy drugs. Alternatively, the rMETase-induced S/G_2 block can be lifted and the cells can become sensitive to M-phase drugs. This approach has significant clinical potential since almost all cancer cell types tested are methionine dependent and arrest in S/G_2 when deprived of methionine with an agent such as rMETase.

MATERIALS AND METHODS

Recombinant Methioninase (rMETase)

Recombinant L-methionine α-deamino-γ-mercaptomethane lyase (methioninase, METase) [EC 4.4.1.11] from *Pseudomonas putida* has been previously cloned and was produced in *Escherichia coli* (AntiCancer, Inc., San Diego, CA). rMETase is a homotetrameric PLP enzyme of 172-kDa molecular mass [52].

FUCCI (Fluorescence ubiquitination cell cycle indicator)

The FUCCI probe was generated by fusing mKO2 (monomeric Kusabira Orange2) and mAG (monomeric Azami Green) to the ubiquitination domains of human Cdt1 and geminin, respectively. These two chimeric proteins, mKO2-hCdt1(30/120) and mAG-hGem(1/110), accumulate reciprocally in the nuclei of transfected cells during the cell cycle, labeling the nuclei of G_1 phase cells red and nuclei of cells in S/G_2 phase green [53].

FUCCI-expressing HeLa cells and MCF-7 cells

Plasmids expressing mKO2-hCdt1 or mAG-hGem (MBL, Nagoya, Japan) were transfected into HeLa cells and MCF-7 cells. HeLa cells were grown in DMEM supplemented with 10% fetal bovine serum and penicillin/streptomycin. MCF-7 were grown in MEM-supplemented with L-glutamine and 10% fetal bovine serum and penicillin/streptomycin [53].

Imaging of FUCCI-expressing cancer cells

Time-lapse images of HeLa and MCF-7 cells stably transfected with FUCCI vectors were acquired using a confocal laser scanning microscope (FV1000; Olympus, Tokyo, Japan) [1, 2, 21].

Cell viability

For cell viability determinations before and after chemotherapy, with and without rMETase, the cells were stained with crystal violet, and the relative number of cells was quantified using ImageJ (NIH, Bethesda, MD).

DEDICATION

This paper is dedicated to the memory of A. R. Moossa, MD.

ACKNOWLEDGEMENTS

This work was supported by National Cancer Institute grant CA132971.

CONFLICTS OF INTEREST

S.L., Q.H. and Y.T. are employees of AntiCancer Inc. S.Y. and R.M.H. are unsalaried associates of AntiCancer Inc. There are no other competing financial interests.

Abbreviations

recombinant methioninase = rMETase; fluorescence ubiquitination cell cycle indicator = FUCCI

REFERENCES

1. Yano S, Zhang Y, Miwa S, Tome Y, Hiroshima Y, Uehara F, Yamamoto M, Suetsugu A, Kishimoto H, Tazawa H, Zhao M, Bouvet M, Fujiwara T, Hoffman RM. Spatial-temporal FUCCI imaging of each cell in a tumor demonstrates locational dependence of cell cycle chemoresponsiveness. Cell Cycle 2014; 13:2110-2119.
2. Yano S, Miwa S, Mii S, Hiroshima Y, Uehara F, Yamamoto M, Kishimoto H, Tazawa H, Bouvet M, Fujiwara T, Hoffman RM. Invading cancer cells are predominantly in G_0/G_1 resulting in chemoresistance demonstrated by real-time FUCCI imaging. Cell Cycle 2014; 13:953-960.
3. Hoffman RM. Altered methionine metabolism, DNA methylation and oncogene expression in carcinogenesis: a review and synthesis. Biochim Biophys Acta Reviews on Cancer 1984; 738:49-87.
4. Goseki N, Yamazaki S, Shimojyu K, Kando F, Maruyama M, Endo M, Koike M, Takahashi H. Synergistic effect of methionine-depleting total parenteral nutrition with 5-fluorouracil on human gastric cancer: A randomized, prospective clinical trial. Jpn J Cancer Res 1995; 86:484-489.
5. Epner DE, Morrow S, Wilcox M, Houghton JL. Nutrient intake and nutritional indexes in adults with metastatic cancer on a Phase I clinical trial of dietary methionine restriction. Nutrition and Cancer 2002; 42:158–166.
6. Hoffman RM, Jacobsen SJ. Reversible growth arrest in simian virus 40-transformed human fibroblasts. Proc Natl Acad Sci USA 1980; 77:7306-7310.
7. Lu S, Epner DE. Molecular mechanisms of cell cycle block by methionine restriction in human prostate cancer cells. Nutrition and Cancer 2000; 38:123-130.
8. Stern PH, Hoffman RM. Enhanced *in vitro* selective toxicity of chemotherapeutic agents for human cancer cells based on a metabolic defect. J Natl Cancer Inst 1986; 76:629-639.
9. Blagosklonny MV. How cancer could be cured by 2015. Cell Cycle 2005; 4:269-78.
10. Blagosklonny MV. Tissue-selective therapy of cancer. Br J Cancer 2003; 89:1147-51.
11. Blagosklonny MV. Matching targets for selective cancer therapy. Drug Discov Today 2003; 8:1104-7.
12. Blagosklonny MV. "Targeting the absence" and therapeutic engineering for cancer therapy. Cell Cycle 2008; 7:1307-12.
13. Blagosklonny MV. Teratogens as anti-cancer drugs. Cell Cycle 2005; 4:1518-21.
14. Blagosklonny MV. Treatment with inhibitors of caspases, that are substrates of drug transporters, selectively permits chemotherapy-induced apoptosis in multidrug-resistant cells but protects normal cells. Leukemia 2001; 15:936-41.
15. Blagosklonny MV. Target for cancer therapy: proliferating cells or stem cells. Leukemia 2006; 20:385-91.
16. Blagosklonny MV. Cancer stem cell and cancer stemloids: from biology to therapy. Cancer Biol Ther 2007; 6:1684-90.
17. Apontes P, Leontieva OV, Demidenko ZN, Li F, Blagosklonny MV. Exploring long-term protection of normal human fibroblasts and epithelial cells from chemotherapy in cell culture. Oncotarget 2011; 2:222-33.
18. Rao B, van Leeuwen IM, Higgins M, Campbel J, Thompson AM, Lane DP, Lain S. Evaluation of an Actinomycin D/VX-680 aurora kinase inhibitor combination in p53-based cyclotherapy. Oncotarget 2010; 1:639-50.
19. Blagosklonny MV. NCI's provocative questions on cancer: some answers to ignite discussion. Oncotarget 2011; 2:1352-67.
20. Blagosklonny MV. Antagonistic drug combinations that select against drug resistance: from bacteria to cancer. Cancer Biol Ther 2007; 6:1013-4.
21. Yano S, Tazawa H, Hashimoto Y, Shirakawa Y, Kuroda S, Nishizaki M, Kishimoto H, Uno F, Nagasaka T, Urata Y, et al. A genetically engineered oncolytic adenovirus decoys and lethally traps quiescent cancer stem-like cells into S/G_2/M phases. Clin Cancer Res 2013; 19:6495-505.
22. Innominato PF, Roche VP, Palesh OG, Ulusakarya A, Spiegel D, Lévi FA. The circadian timing system in clinical oncology. Ann Med. 2014;46:191-207.
23. Wang X, Pan L, Mao N, Sun L, Qin X, Yin J. Cell-cycle synchronization reverses Taxol resistance of human ovarian cancer cell lines. Cancer Cell Int 2013;13:77.
24. Chandrasekaran B, Kute TE, Duch DS. Synchronization of cells in the S phase of the cell cycle by 3'-azido-3'-deoxythymidine: implications for cell cytotoxicity. Cancer Chemother Pharmacol 1995;35:489-95.
25. Kufe DW, Egan EM, Rosowsky A, Ensminger W, Frei E

3rd. Thymidine arrest and synchrony of cellular growth *in vivo*. Cancer Treat Rep 1980;64:1307-17.

26. Vogler WR, Kremer WB, Knospe WH, Omura GA, Tornyos K. Synchronization with phase-specific agents in leukemia and correlation with clinical response to chemotherapy. Cancer Treat Rep 1976;60:1845-59.
27. Morris CM, Fitzgerald PH. An evaluation of high resolution chromosome banding of hematologic cells by methotrexate synchronization and thymidine release. Cancer Genet Cytogenet 1985;14:275-84.
28. Moran RE, Straus MJ. Synchronization of L1210 leukemia with hydroxyurea infusion and the effect of subsequent pulse dose chemotherapy. Cancer Treat Rep 1980;64:81-6.
29. Dethlefsen LA, Sorensen SP, Riley RM. Effects of double and multiple doses of hydroxyurea on mouse duodenum and mammary tumors. Cancer Res 1975;35:694-9
30. Finzi L, Kraemer A, Capron C, Noullet S, Goere D, Penna C, Nordlinger B, Legagneux J, Emile JF, Malafosse R. Improved retroviral suicide gene transfer in colon cancer cell lines after cell synchronization with methotrexate. J Exp Clin Cancer Res 2011;30:92.
31. Keir ST, Friedman HS, Reardon DA, Bigner DD, Gray LA. Mibefradil, a novel therapy for glioblastoma multiforme: cell cycle synchronization and interlaced therapy in a murine model. J Neurooncol 2013;111:97-102.
32. Keyomarsi K, Sandoval L, Band V, Pardee AB. Synchronization of tumor and normal cells from G1 to multiple cell cycles by lovastatin. Cancer Res 1991;51:3602-9.
33. Javanmoghadam-Kamrani S, Keyomarsi K. Synchronization of the cell cycle using lovastatin. Cell Cycle 2008;7:2434-40.
34. Huang X, Di Liberto M, Jayabalan D, Liang J, Ely S, Bretz J, Shaffer AL 3rd, Louie T, Chen I, Randolph S, Hahn WC, Staudt LM, Niesvizky R, Moore MA,Chen-Kiang S. Prolonged early G(1) arrest by selective CDK4/CDK6 inhibition sensitizes myeloma cells to cytotoxic killing through cell cycle-coupled loss of IRF4. Blood 2012;120:1095-106.
35. Vassilev LT. Cell cycle synchronization at the G_2/M phase border by reversible inhibition of CDK1. Cell Cycle 2006;5:2555-6.
36. Dong XF, Berthois Y, Dussert C, Isnardon D, Palmari J, Martin PM. Mode of EGF action on cell cycle kinetics in human breast cancer cell line MCF-7: some evidence that EGF acts as a "progression factor". Anticancer Res 1992;12:2085-92.
37. Hambek M, Werner C, Baghi M, Gstöttner W, Knecht R. Enhancement of docetaxel efficacy in head and neck cancer treatment by G0 cell stimulation. Eur J Cancer 2007;43:1502-7.
38. Hambek M, Werner C, Baghi M, Gstöttner W, Knecht R. Prestimulation of head and neck cancer cells with growth factors enhances treatment efficacy. Anticancer Res 2006;26:1091-5.
39. Grdina DJ, Meistrich ML, Meyn RE. Cell synchrony techniques. A comparison of methods. In: Techniques in Cell Cycle Analysis. Gray JW and Darzynkiewicz A (eds). Humana Press Inc., Clifton, NJ, 1987;367-403.
40. Davis PK, Ho A, Dowdy SF. Biological methods for cell-cycle synchronization of mammalian cells. Biotechniques 2001;30:1322-6, 1328, 1330-1.
41. Merril GF. Cell synchronization. Methods Cell Biol 1998;57:229-249.
42. Amon A. Synchronization procedures. Methods Enzymol 2002;351:457-67.
43. Hoffman, R.M. and Erbe, R W. High *in vivo* rates of methionine biosynthesis in transformed human and malignant rat cells auxotrophic for methionine. Proc. Natl. Acad. Sci. USA 1976; 73:1523-7.
44. Hoffman, R.M., Jacobsen, S J. and Erbe, R.W. Reversion to methionine independence by malignant rat and SV40-transformed human fibroblasts. Biochem. Biophys. Res. Commun. 1978; 82:228-34.
45. Hoffman, R.M., Jacobsen, S.J. and Erbe, R.W. Reversion to methionine independence in simian virus 40-transformed human and malignant rat fibroblasts is associated with altered ploidy and altered properties of transformation. Proc Nat!Acad Sci USA 1979; 76:I313-7.
46. Coalson, D.W., Mecham, J.O., Stem, P.H., and Hoffman, R.M. Reduced availability of endogenously synthesized methionine for S-adenosylmethionine formation in methionine-dependent cancer cells. Proc Nat! Acad Sci USA 1982; 79:4248-51 .
47. Stem, P.H., Mecham, 1.0., Wallace, C.D. and Hoffman, R.M. Reduced free-methionine in methionine-dependent SV40-transformed human fibroblasts synthesizing apparently normal amounts of methionine. J Cell Physiol l983; 117:9-14.
48. Mecham, 1.0., Rowitch, D., Wallace, C.D., Stem, P.H. and Hoffman, R.M. The metabolic defect of methionine dependence occurs frequently in human tumor cell lines. Biochem, Biophys Res Commun 1983; 117:429-34.
49. Stem, P.H., Wallace, C.D. and Hoffman, R.M. Altered methionine metabolism occurs in all members of a set of diverse human tumor cell lines. J Cell Physiol 1984; I I 9:29-34.
50. Stem, P.H., and Hoffman, R.M. Elevated overall rates of transmethylation in cell lines from diverse human tumors. *In Vitro* I984; 20:663-70.
51. Tan, Y., Xu, M., and Hoffman, R.M. Broad selective efficacy of recombinant methioninase and polyethylene glycol-modified recombinant methioninase on cancer cells *in vitro*. Anticancer Res 2010; 30:1041-6.
52. Tan Y, Xu M, Tan X, Tan X, Wang X, Saikawa Y, Nagahama T, Sun X, Lenz M, Hoffman RM. Overexpression and large-scale production of recombinant methionine-α-deamino-γ-mercaptomethane-lyase for novel

anticancer therapy. Protein Expression and Purification 1997; 9:233-245.

53. Sakaue-Sawano A, Kurokawa H, Morimura T, Hanyu A, Hama H, Osawa H, Kashiwagi S, Fukami K, Miyata T, Miyoshi H, et al. Visualizing spatiotemporal dynamics of multicellular cell cycle progression. Cell 2008; 132:487-98.

REPORT

Cell Cycle 13:6, 953–960; March 15, 2014; © 2014 Landes Bioscience

Invading cancer cells are predominantly in G_0/G_1 resulting in chemoresistance demonstrated by real-time FUCCI imaging

Shuya Yano[1,2,3], Shinji Miwa[1,2], Sumiyuki Mii[1,2], Yukihiko Hiroshima[1,2], Fuminari Uehara[1,2], Mako Yamamoto[1,2], Hiroyuki Kishimoto[3], Hiroshi Tazawa[4], Michael Bouvet[2], Toshiyoshi Fujiwara[3], and Robert M Hoffman[1,2,*]

[1]AntiCancer, Inc; San Diego, CA USA; [2]Department of Surgery; University of California, San Diego; San Diego, CA USA; [3]Department of Gastroenterological Surgery; Okayama University Graduate School of Medicine, Dentistry, and Pharmaceutical Sciences; Okayama, Japan; [4]Center for Innovative Clinical Medicine; Okayama University Hospital; Okayama, Japan

Keywords: cancer invasion, cell cycle kinetics, fluorescent proteins, FUCCI, 3D, Gelfoam® histoculture, confocal laser microscopy, real-time imaging

Abbreviations: FUCCI, fluorescence ubiquitination cell cycle indicator; CLSM, confocal laser scanning microscopy

Invasive cancer cells are a critical target in order to prevent metastasis. In the present report, we demonstrate real-time visualization of cell cycle kinetics of invading cancer cells in 3-dimensional (3D) Gelfoam® histoculture, which is in vivo-like. A fluorescence ubiquitination cell cycle indicator (FUCCI) whereby G_0/G_1 cells express a red fluorescent protein and $S/G_2/M$ cells express a green fluorescent protein was used to determine the cell cycle position of invading and non-invading cells. With FUCCI 3D confocal imaging, we observed that cancer cells in G_0/G_1 phase in Gelfoam® histoculture migrated more rapidly and further than cancer cells in $S/G_2/M$ phases. Cancer cells ceased migrating when they entered $S/G_2/M$ phases and restarted migrating after cell division when the cells re-entered G_0/G_1. Migrating cancer cells also were resistant to cytotoxic chemotherapy, since they were preponderantly in G_0/G_1, where cytotoxic chemotherapy is not effective. The results of the present report suggest that novel therapy targeting G_0/G_1 cancer cells should be developed to prevent metastasis.

Introduction

Cancer cell invasion is the prelude for metastasis.[1-3] Therefore, targeting invading cancer cells is critical to prevent metastasis.[4-6] However, in order to target invading cancer cells, it is necessary to determine their cell cycle phase, since most cytotoxic chemotherapy targets $S/G_2/M$ cells. Sakaue-Sawano et al.[7] have utilized oscillating proteins that specifically mark cell cycle phases in order to image cell cycle kinetics in a system they term FUCCI (fluorescence ubiquitination cell cycle indicator). Individual G_1 phase nuclei are red, and those in $S/G_2/M$ phases are green in the FUCCI system.

For tracking invading cancer cells, 3-dimensional culture is indispensable.[8-12] Collagen sponge-gel histoculture was developed by Leighton.[13] Placing cells in histoculture enables them to form 3-dimensional structures.[13] Because of its architectural resemblance to native tissue, sponge gel histoculture represents a unique in vivo-like model to study cancer-cell behavior.[14] For example, Leighton observed that when C3HBA mouse mammary adenocarcinoma cells were grown on sponge-matrix histoculture, the cells aggregated similar to the original in vivo tumor. Distinct structures were formed within the tumors, such as lumina and stromal elements, with some of the glandular structures similar to the original tumor. When Leighton cultured hepatoma cells in sponge-matrix culture, they behaved differently from the normal liver cells and grew in a loosely packed arrangement as opposed to normal liver cells.[15]

We have further developed sponge gel histoculture using Gelfoam® to grow tumors,[16,17] nerves growing from stem cells,[18-20] hair follicles,[21] skin with growing hair,[22] and Margolis et al.[23] have used Gelfoam® to culture lymphoid tissue.

In the present report, we use confocal imaging and Gelfoam® collagen sponge gel histoculture of human stomach cancer cells expressing FUCCI to determine the cell cycle position of invasive and non-invasive cancer cells and their sensitivity to cytotoxic chemotherapy. The implication of these results for the study and treatment of metastasis are discussed.

*Correspondence to: Robert M Hoffman; Email: all@anticancer.com
Submitted: 12/19/2013; Accepted: 01/12/2014; Published Online: 01/20/2014
http://dx.doi.org/10.4161/cc.27818

Results and Discussion

Gelfoam® 3-dimensional histoculture enables real-time tracking of FUCCI-expressing invading and non-invading cancer cells

In Gelfoam® histoculture, invading cancer cells were mostly in G_0/G_1 phase, while non-invading cells were mostly in $S/G_2/M$ phases (**Fig. 1A**). The cell cycle distribution of invading cells was 84.3% in G_0/G_1 phase. In contrast, in non-invading cells at the tumor surface, the percentage of cells in $S/G_2/M$ was 67.5% (**Fig. 1A**). Cancer cells located at the invading area of a Gelfoam® tumor could be tracked for at least 3 days (**Fig. 1B; Video S1**). Some invading cancer cells migrated along the structure of the Gelfoam® (**Fig. 1C; Video S1**); the other cancer cells spread inside the structure of the Gelfoam® (**Fig. 1C; Video S1**).

Cell cycle distribution of the invading versus non-invading areas of tumors in Gelfoam® histoculture

Cancer cells at the invading edge of the tumor moved along the Gelfoam® structures and were mostly in G_0/G_1 (94.0 ± 4.9%) (**Fig. 2A**). In contrast, cancer cells at the center of the tumor fluoresced red, yellow, and green and were thus distributed throughout the cell cycle (S phase; 23.7 ± 18.0%; G_2/M phase; 30.5 ± 16.6%) (**Fig. 2A**). Cancer cells in G_0/G_1 phase contacted each other (**Fig. 2B**).

Cancer cells in G_0/G_1-phase are motile compared with $S/G_2/M$-phase cancer cells in Gelfoam® histoculture

Cancer cells in G_0/G_1 phase migrated more than cancer cells in $S/G_2/M$ at the tumor edge in Gelfoam®: G_0/G_1 phase, 66.5 ± 31.2 μm/48 h; $S/G_2/M$ phase, 21.8 ± 14.0 μm/48 h; $P < 0.0001$ (**Fig. 3A, C, and D**). Moreover, single cancer cells in G_0/G_1 phase migrated significantly further (up to 200 μm over 48 h) than those in $S/G_2/M$ phases (up to 90 μm over 48 h) (**Fig. 3B and D; Video S2**).

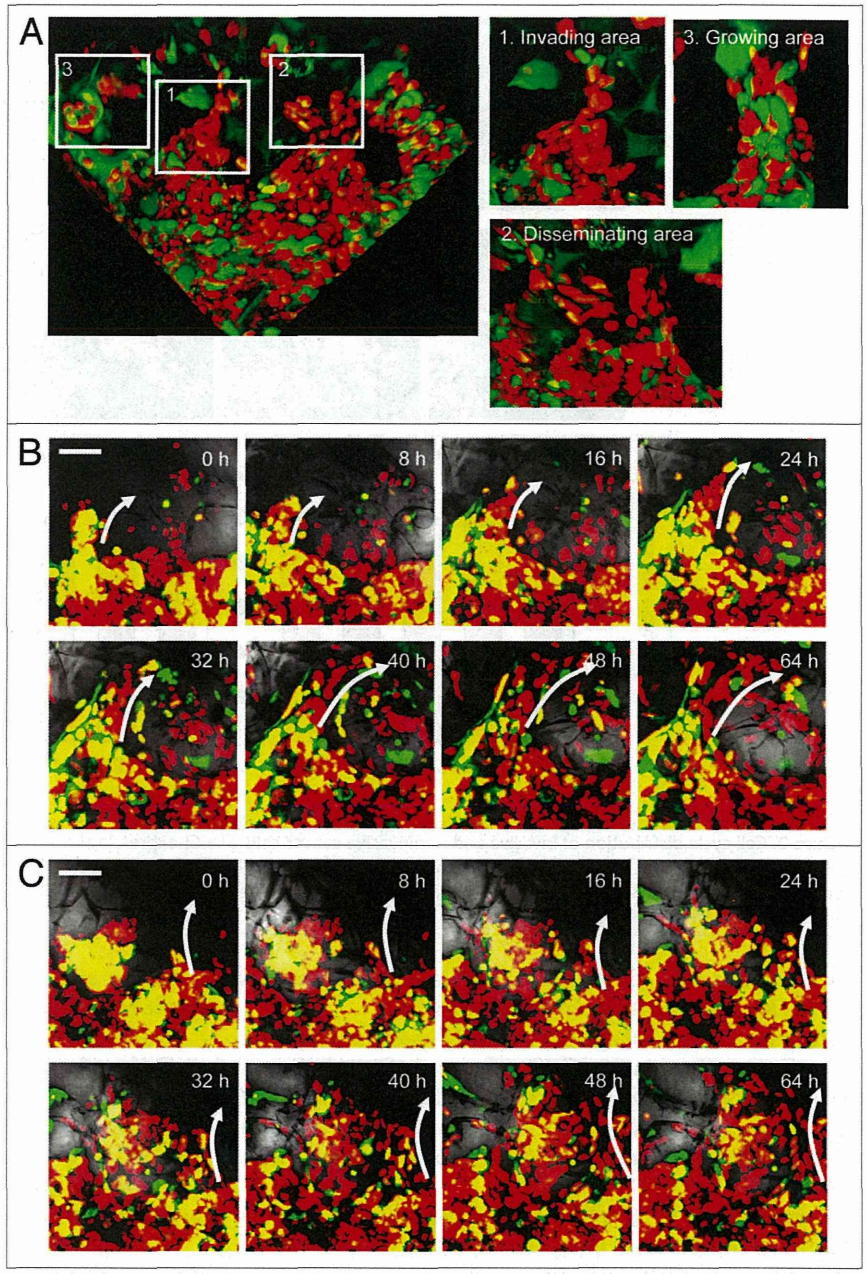

Figure 1. Gelfoam® histoculture enables tracking of the cell cycle kinetics of invading and non-invading FUCCI-expressing cancer cells. All images were acquired with confocal laser scanning microscopy (CLSM) using the FV1000 (Olympus). FUCCI-expressing cancer cells in G_0/G_1, S, or G_2/M phases appear red, yellow, or green, respectively. FUCCI-expressing cancer cells (2×10^7) were placed on Gelfoam® (1 × 1 cm) in RPMI 1640 medium. (**A**) Gelfoam® culture enables cancer cells to be visualized at different locations in tumor-like structures (left). High magnification view (right). (**B**) High-magnification real-time images of cancer cells invading from a tumor on Gelfoam® for 64 h. Arrows show the direction of invading cancer cells. (**C**) High-magnification real-time images of cancer cells disseminating from a tumor on Gelfoam® for 64 h. Arrows show the direction of invading cancer cells. Scale bars: 100 μm.